Metastable states and macroscopic quantum tunneling in a cold atom Josephson ring

Dmitry Solenov* and Dmitry Mozyrsky†

Theoretical Division (T-4), Los Alamos National Laboratory, Los Alamos, NM 87545, USA
(Dated: September 18, 2009)

We study macroscopic properties of a system of weakly interacting neutral bosons confined in a ring-shaped potential with a Josephson junction. We derive an effective low energy action for this system and evaluate its properties. In particular we find that the system possesses a set of metastable current-carrying states and evaluate the rates of transitions between these states due to macroscopic quantum tunneling. Finally we discuss signatures of different metastable states in the time-of-flight images and argue that the effect is observable within currently available experimental technique.

PACS numbers: 03.75.Kk, 37.10.Gh, 85.25.Cp

Macroscopic Quantum Tunneling (MQT) is undoubtedly one of the most remarkable manifestations of macroscopic quantum coherence, a property intrinsic to superconductors and Bose-Einstein Condensate (BEC) systems. The most well studied system exhibiting MQT is the so-called phase qubit, a superconducting loop containing a Josephson junction, where MQT occurs between metastable current-carrying states of the Cooper pair condensate in the loop [1, 2]. The main mechanisms controlling these metastable states and the MQT arise from an interplay between several factors, such as Josephson, inductive, and charging energies, as well as dissipation due to shunting resistances and/or quasiparticle excitations. The Josephson and the inductive energies form an effective potential for the flux-phase variable (i.e., the phase difference across the Josephson junction), while the charging energy (resulting from plasma oscillations due to the Coulomb interactions between electrons) gives rise to the effective kinetic energy for the phase [2, 3]. Dissipation is also known to play a critical role in MQT dynamics, leading to a substantial slow-down in tunneling rates [4, 5] as well as to the localization of the magnetic flux in the case of symmetric double well effective potential (realizable by applying a 1/2 magnetic flux quantum through the loop) [6, 7].

In this Letter we consider dynamics and properties of a phase qubit-like (Josephson ring) device based on a BEC of neutral particles. Contrary to the conventional superconductor-based devices, these systems did not receive much attention in literature, - presumably due to lack of their experimental realizations in the past. Our interest in such systems, however, is *not* purely academic: advances in cold atom trapping, such as the recently demonstrated "painted potential" technique [8], open a clear path for the realization and development of such phase qubits. As we will show below, these cold atom per-
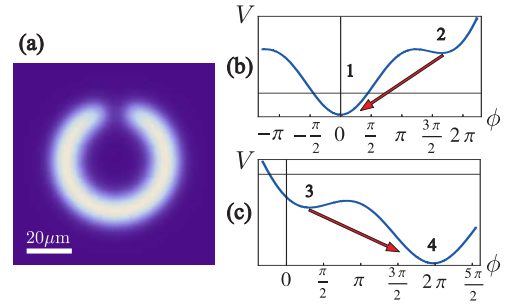
*E-mail: solenov@lanl.gov
†E-mail: mozyrsky@lanl.gov

FIG. 1: (Color online) (a) The system of interest: Density profile of a BEC in a "painted potential", i.e., a ring with a tunnel junction (see Ref. [8] for comparison with actual experimental photographs). (b) and (c) Effective potentials as a functions of phases across the Josephson junctions for two cases: (b) $\Omega = 0$, $\alpha = 5.8$ and (c) $\Omega \neq 0$, $\alpha = 5.8$ and $\phi_0 = 5.8$.

sistent current devices posses a number of properties similar to their superconducting counterparts. These properties, however, are controlled by rather different physical mechanisms, which rely not on particles' charge (like inductive and charging energies of the in superconducting devices), but on the effects of quantization due to the finite size of the system. Indeed, while for superconductors the phase (Goldstone) mode is gapped due to plasmon oscillations, it is gapless for the neutral particles interacting through a short range potential. As a result, the phase dynamics for the latter systems is susceptible to the long-range fluctuations and is strongly affected by the system's dimensionality, geometry of the traps, etc.

We consider a BEC confined in a ring-shaped potential containing a single cut, i.e., a tunnel (Josephson) junction, see Fig. 1(a). We derive an effective action for the phase difference across the Josephson junction. Dynamics described by this action strongly depends on the system's size (i.e., the ring's circumference), and is dramatically different in the two limiting cases, i.e., for small and large BEC rings. In the latter case dynamics of the phase ϕ across the junction corresponds to that of an overdamped particle, diffusing in a periodic potential

(due to the Josephson energy at the junction, see below). In the former case the "phase-particle" is underdamped and moves in the potential, which is a sum of Josephson energy ($\sim \cos \phi$) and effective inductive energy ($\sim \phi^2$). The inductive energy term is of quantum origin: It arises due the kinetic energy of the BEC particles confined in the ring. The competition between Josephson and the effective inductive energies gives rise to the formation of metastable current-carrying states, i.e., with $\phi \neq 0$. We obtain criteria for the formation of these states and discuss means of their control and possibility of their realization in cold atom systems. We analyze MQT rates from these states as a function of system's parameters for stationary and for rotating potentials. Finally we outline signatures of these current-carrying states in time-of-flight experiments.

The Hamiltonian for the system of interest is given by

$$H = \int_0^L dx \, \hat{\psi}^\dagger(x) \left[-\frac{\nabla^2}{2m} + \frac{\lambda}{2} \hat{\psi}^\dagger(x)\hat{\psi}(x) + V(x) \right] \hat{\psi}(x),$$
(1)

where potential $V(x)$ describes the tunnel barrier and the system is assumed to be one dimensional [9] with periodic boundary conditions. Here and in the following we use units with $\hbar = 1$ and $k_B = 1$, unless stated otherwise. We would like to derive an effective low energy action for the system described by the Hamiltonian in Eq. (1). This can be carried out as follows. In the absence of the potential barrier $V(x)$ this action is readily obtained by representing Bose field operators in terms of hydrodynamic variables as $\psi = \sqrt{\rho + \delta\rho} \, e^{i\varphi}$, where $\rho = N/L$ and N is total number of atoms in the ring. In that case the linearization with respect to the small density variations $\delta\rho$ yields an effective phonon Lagrangian in the long wavelength limit [10]. In the phase representation it reads

$$\mathcal{L}_0 = \int_0^L dx \frac{1}{2\lambda} \left[(\partial_\tau \varphi)^2 + c^2 (\partial_x \varphi)^2 \right],$$
(2)

where c is sound velocity for an equivalent infinite system ($c = (\rho\lambda/m)^{1/2}$ in the weak coupling limit). Here and in the following we use imaginary (Matsubara) time representation. The spectrum of the phonons is discrete due to the finite size of the system, with energy spacing between the adjacent levels $\Delta E = 2\pi c/L$. If the barrier is sufficiently high, the inclusion of the tunnel barrier potential $V(x)$ changes the functional dependence of the Lagrangian density on φ only locally. That is, the BEC Lagrangian density in the region with $V(x) = 0$ is still given by Eq. (2), supplemented by the appropriate boundary conditions at the barrier (see below). For the high potential barrier transitions across the barrier can be described by the usual hopping term $\sim [\psi^\dagger(0)\psi(L) + \psi^\dagger(L)\psi(0)]$ and therefore the effective action can be cast in the form

$$S = \int d\tau \left[\mathcal{L}_0 - \rho t \cos \phi(\tau) \right],$$
(3)

where $\phi = \varphi(0) - \varphi(L)$ is the phase difference across the junction and t is the transmission coefficient. Obviously the value of t depends on the shape of the potential barrier as well as it accounts for the depletion of the density near the barrier. Moreover, it may depend on the interactions between particles and their density [11]. However, if the height of the barrier V_0 is large compared to the interaction energy $\lambda\rho$, this dependence can be neglected, and, as a rough estimate, one can use the standard semiclassical expression for the rectangular barrier, $t \sim (1/md) \exp\left[-d(2mV_0)^{1/2}\right]$, where d is the width of the barrier. Furthermore, Eqs. (2, 3) are applicable only when Josephson energy per particle $\rho t/N$ is small compared to the level spacing ΔE, i.e., for $c \gg t$; otherwise the presence of the barrier significantly affects the quasiparticle (i.e. phonon) states inside the ring and the weak link picture is no longer valid. In this weak link limit the supercurrent at $x = 0$ and $x = L$ is vanishingly small, and therefore Eq. (3) must be supplemented by the boundary conditions $\partial_x \varphi(0, \tau) = \partial_x \varphi(L, \tau) = 0$.

The action given by Eqs. (2, 3) can be reduced to a local action by integrating out the $\varphi(x, \tau)$ field everywhere except $x = 0$ and $x = L$. This is accomplished by introducing the functional δ-function according to

$$Z = \prod_\omega \int \mathcal{D}\phi \mathcal{D}\varphi e^{-S} \delta[\phi(\omega) - \varphi(0, \omega) + \varphi(L, \omega)],$$
(4)

and using identity $\delta(a) = (2\pi)^{-1} \int dz \exp(iza)$. The fields φ and z can then be integrated out (note that in doing so one should expand field $\varphi(x, \tau)$ in $\cos(\pi n x/L)$, thus satisfying the boundary conditions above). After some calculation we obtain that the partition function takes the form $Z = \int \mathcal{D}\phi \exp(-S_{\text{eff}})$, where

$$S_{\text{eff}} = \int \frac{d\omega}{2\pi} |\phi(\omega)|^2 \frac{c\,\omega}{4\lambda \tanh\left(\frac{\omega L}{2c}\right)} - \rho t \int d\tau \cos \phi(\tau).$$
(5)

Effective action in Eq. (5) is similar to that for an impurity in the Luttinger liquid [12]. The first term of the right-hand side is different due to the finite length of the ring. Indeed, for sufficiently large ring the first term is proportional to $|\omega|$ and the action is that of a dissipative particle in a periodic potential. In the opposite small ring limit, the first term in Eq. (5) yields

$$\int d\tau \left[(L/24\lambda)\dot{\phi}^2(\tau) + (\rho/2mL)\phi^2(\tau) \right],$$
(6)

where the effective kinetic energy term describes the lowest BEC mode, that is, motion of the BEC as a whole, and the last "inductive" term arises due to the kinetic energy of the BEC particles in the ring. Together with the cosine term in Eq. (5) this ϕ^2 term provides effective potential energy for the "phase particle". This potential may have one (at $\phi = 0$) or more (at $\phi \neq 0$) local minima. The $\phi \neq 0$ minima correspond to the

metastable states carrying non-zero current. The shape of such effective potential can be conveniently characterized in terms of the dimensionless parameter $\alpha = mtL$. For $\alpha = \alpha_1 \approx 4.60$ the first two metastable minima appear at $\phi \approx \pm 1.43\pi$. Two more metastable states appear when $\alpha > \alpha_2 \approx 10.95$, and so on. Furthermore, the effective potential can be modified by rotating the "painted potential". As a result the potential energy of the superfluid in the rotating reference frame changes by $-M\Omega$, where Ω is angular frequency of rotation and M is angular momentum of the superfluid (in the stationary frame) [10], and therefore the effective potential $V(\phi)$ can be cast in the form

$$V^{\text{eff}}(\phi) = \rho t \left[\frac{(\phi - \phi_0)^2}{2\alpha} - \cos\phi \right], \qquad (7)$$

where $\phi_0 = 2\pi I \Omega$ (here I is the moment of inertia of the superfluid per atom, $I \simeq mL^2$). Such $V^{\text{eff}}(\phi)$ is equivalent to that of a Josephson flux qubit, i.e., a superconducting loop with a Josephson junction in a magnetic field [7]. For $\phi_0 = \pi$ effective potential $V^{\text{eff}}(\phi)$ is a symmetric double well, while for $\phi_0 > \pi$ the minimum close to 0 becomes metastable and then, upon further increase of Ω, disappears completely for $\phi_0 > \phi_0^{\text{cr}} = [\sqrt{\alpha^2-1} + |\cos^{-1}(-1/\alpha)|]/\alpha$.

Note that in Eq. (7) the particle density controls only the overall strength of the effective potential, but not its relative shape. The latter depends only on the parameter α, which is determined by the properties of the "painted potential", but not by the number of particles in the system. This fact is rather advantageous from the experimental point of view: While the number of particles in the system typically obeys Poissonian statistics and therefore it can significantly fluctuate in different experimental runs, the form of the painted potential (i.e., the value of parameter α determining the onset of the metastability) is easy to control with sufficiently high precision.

Transitions between different minima of the effective potential in Eq. (7) are driven by thermal and quantum fluctuations. The former mechanism dominates at sufficiently high temperatures, exceeding frequency of small Josephson oscillations in a given well. Note that in the metastable region, i.e. for $mtL \geq 1$, this frequency is of the order of the spacing between quasiparticle energy levels, ΔE. For the system of ^{87}Rb atoms $L \simeq 0.2\,\text{mm}$ and $\rho^{3D} \sim 10^{12}\,\text{cm}^{-3}$, e.g. Ref. [8], $T^* \sim \Delta E \sim 0.2\,\text{nK}$. Thus, above T^* the rate of transitions is determined by the thermal activation rate $\sim \exp(-V_0^{\text{eff}}/T)$, where V_0^{eff} is the height of the effective potential barrier in Eq. (7). In the following we evaluate transition rates for two cases: (I) For a system in the first metastable state, i.e., for $\alpha_1 < \alpha < \alpha_2$ and $\Omega = 0$, e.g. Fig. 1(b); (II) For the rotating system ($\Omega \neq 0$), when the initially global minimum at $\phi = 0$ becomes metastable, i.e., for $\pi \leq \phi_0 \leq \phi_0^{\text{cr}}$, e.g., Fig. 1(c). In the former case the rate of thermally

activated transition Γ_T is given by

$$\ln \frac{\Gamma_0}{\Gamma_T} = \frac{0.86\rho}{mLT}(\alpha - \alpha_1)^{3/2}, \qquad (8)$$

while for the latter case

$$\ln \frac{\Gamma_0'}{\Gamma_T'} = \frac{1.89\rho}{mLT}(\alpha^2 - 1)^{-1/4}(\phi_0^{\text{cr}} - \phi_0)^{3/2}. \qquad (9)$$

For the order of magnitude estimate both pre-exponential factors Γ_0 and Γ_0' can be taken as frequency of small Josephson oscillations $\sim \Delta E$ [13], while the height of the effective potential barrier $V_0^{\text{eff}} \sim \rho/(mL)$ in Eqs. (8, 9) is of the order of 10 nK (here and in the following we use the same values for the system's parameters as above; see also Ref. [8]). Thus we expect that thermally activated transition rates of the order of $1 - 10$ Hz are readily observable at temperatures below 10 nK.

For temperatures below $T^* \sim 0.2$ nK thermal activation mechanism becomes ineffective and transitions are driven by quantum fluctuations, i.e., by the MQT. The rate of the MQT can be computed by evaluating Euclidean action over the classical instanton trajectory $\Gamma = \Gamma_0 \exp[-S(\phi_{cl})]$ [14]. Measurable MQT rates can be found near the spinodal instabilities of the metastable states, i.e., when the effective potential barriers are relatively small. In this regime one can expand the effective potentials around the local minima (state 2 in Fig. 1(b), e.g. case (I), and state 3 in Fig. 1(c), case (II)) up to the cubic terms in $(\phi - \phi_{\text{min}})$. The kinetic energy, i.e., the first term in Eq. (5) minus its value at $\omega = 0$ (the second term in Eq. (6)), is non-local in Matsubara time τ and therefore is difficult to be dealt with exactly. For, $\alpha_1 - \alpha \ll 1$, however, the instanton trajectory $\phi_{cl}(\tau)$ contains only small frequencies. In this limit the kinetic energy is local, e.g., the first term in Eq. (6). In the non-local $\alpha_1 - \alpha \geq 1$ regime we use variational approach by choosing $\phi_{cl}(\tau) = \phi_{cl}^0 \exp(-|\tau|/\Delta\tau)$, where ϕ_{cl}^0 and $\Delta\tau$ are variational parameters. The results for $\Omega = 0$, i.e., case (I), are

$$\ln \frac{\Gamma_0}{\Gamma_Q} = \eta \begin{cases} 2.07(\alpha - \alpha_1)^{5/4} & \alpha - \alpha_1 \ll 1 \\ 1.63(\alpha - \alpha_1) & \alpha - \alpha_1 \geq 1 \end{cases}, \qquad (10)$$

where $\eta = \sqrt{\rho/(m\lambda)}$ and the pre-exponential factor Γ_0 is again of the order of ΔE [15]. Evaluation of the MQT for the rotating system, i.e., case (II), gives

$$\ln \frac{\Gamma_0'}{\Gamma_Q'} = \eta \begin{cases} 1.65(\alpha^2-1)^{-3/8}(\phi_0^{\text{cr}} - \phi_0)^{5/4} & \phi_0^{\text{cr}} - \phi_0 \ll 1 \\ 1.88(\alpha^2-1)^{-9/8}(\phi_0^{\text{cr}} - \phi_0) & \phi_0^{\text{cr}} - \phi_0 \geq 1 \end{cases}. \qquad (11)$$

Note that the exponents for the MQT rates in Eqs. (10, 11) are not proportional to the system's size or its total number of particles. e.g. Ref. [16]. Indeed, while the effective mass, e.g. Eq. (6), is proportional to L, the height of the effective potential barrier scales as L^{-1}.
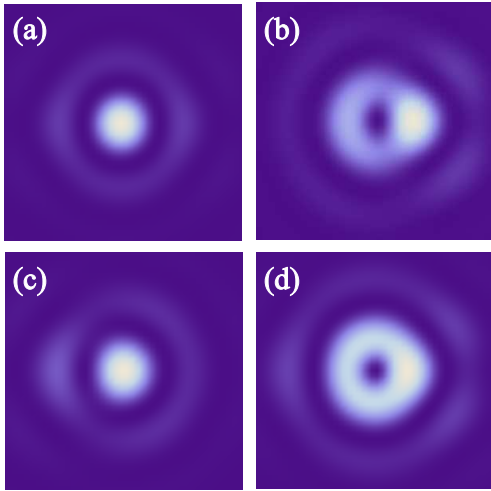
FIG. 2: (Color online) Calculated TOF measurement outcomes for: (i) Transitions from the metastable current state $2 \rightarrow 1$, Fig. 1, with $\Omega = 0$. Observation of (a) corresponds to state "1" and (b)— to state "2". (ii) Transitions to the current-carrying state in $(\Omega \neq 0)$ case. Image (c) corresponds to state "3" and (d) — to state "4".

The value of parameter η in Eqs. (10, 11) for the experiments in Ref. [8] is ~ 300 and therefore fine tuning of parameters is needed in order to obtain reasonable MQT rates. While this fact presents a formidable difficulty in some MQT proposals, e.g. Ref. [16], it seems that such fine tuning is relatively simple for the present system. Indeed, the value of parameter ϕ_0 is determined solely by the system's geometry and by the frequency of rotation, but not by the density, and therefore can be controlled with desired precision. Moreover, the value of η can be reduced by decreasing the cross-section of the ring [17], or by increasing the scattering length, i.e., the value of λ, via the Feshbach resonance.

Finally we briefly discuss the signatures of the current-carrying metastable states in the Time-Of-Flight (TOF) measurements. As well known, after the trapping potential is turned off, at sufficiently long times of expansion the resulting BEC state corresponds to the Fourier transform of the initial state in the trap. In Fig. 2 we present numerical Fourier transforms of the initial states that have same particle density $|\psi_0(r, \theta)|^2$ shown in Fig. 1(a), but multiplied by different phase factors $\exp{(in\theta)}$, where phases $2\pi n$ correspond to the values of ϕ in minima 1 through 4 of the effective potentials in Fig. 1(b) and Fig. 1(c). That is, $n = 0$ for the state 1, while $n \simeq 0.75$ for the state 2, and so on. The main distinction between Fourier images of states with $n \sim 0$ and with $n \sim 1$ is clear: While the former case corresponds to the momentum distributions mainly concentrated at the origin, e.g. Figs. 2(a) and 2(c), in the later case the distribution is *ring-like*, e.g. Figs. 2(b) and 2(d) [18].

In summary, we have proposed a novel BEC based qubit-like device and theoretically studied its properties. We have identified a set of macroscopic metastable states that such system is expected to exhibit under certain conditions and evaluated transition rates between these states. We have discussed signatures of these states in the standard TOF measurements and argue that the effects considered in this paper can be readily observed in contemporary cold atom systems.

[1] M. Tinkham, *Introduction to Superconductivity* (Dover Publications; 2nd Edition, 2004) and references therein.
[2] U. Weiss, *Quantum Dissipative Systems* (World Scientific, 1999).
[3] V. Ambegaokar, U. Eckern and G. Schon, Phys. Rev. Lett **48**, 1745 (1982).
[4] A. O. Caldeira and A. J. Leggett, Phys. Rev. Lett. **46**, 211 (1981).
[5] D. Solenov and D. Mozyrsky, Phys. Rev. Lett. **100**, 150402 (2008).
[6] A. J. Leggett, S. Chakravarty, A. T. Dorsey. M. P. Fisher, A. Garg, and W. Zwerger, Rev. Mod. Phys. **67**, 1 (1987).
[7] Y. Makhlin, G. Schon, and A. Shnirman, Rev. Mod. Phys. **73**, 357 (2001).
[8] K. Henderson, C. Ryu, C. MacCormick and M. G. Boshier, New J. Phys. **11**, 043030 (2009).
[9] Indeed in experiments of Ref. [8] the transverse size of the ring is of the order of the BEC healing length.
[10] E. M. Lifshitz and L. P. Pitaevskii, *Statistical Physics II* (Pergamon Press, 1980).
[11] F. Dalfovo, L. Pitaevskii, amd S. Stringari, Phys. Rev. A **54**, 4213 (1996); I. Zapata, F. Sols and A. J. Leggett, Phys. Rev. A **57**, R28 (1998).
[12] C. L. Kane and M. P. A. Fisher, Phys. Rev. Lett. **68**, 1220 (1992).
[13] D. A. Gorokhov and G. Blatter, Phys. Rev. B **56**, 3130 (1997).
[14] S. Coleman, *Aspects of Symmetry* (Cambridge University Press, 1985).
[15] In $\alpha - \alpha_1 \ll 1$ case a more detailed evaluation gives $\Gamma_0 = 9.21(c/L)[S(\phi_{cl})/\hbar]^{1/2}(\alpha - \alpha_1)^{1/4}$; see Ref. [16].
[16] M. Ueda and A. J. Leggett, Phys. Rev. Lett. **80**, 1576 (1998).
[17] In Eqs. (10, 11) ρ and λ can be expressed in term of the "normal" 3D values as $\rho = \rho^{3D}S$ and $\lambda = \lambda^{3D}/S$, where S is the cross-section area. For Ref. [8] we estimate the cross-section area as $S \simeq \pi D^2/4$, where $D \simeq 10 \ \mu m$.
[18] Recall that a 2D Fourier transform of $\psi_0(r, \theta) = \delta(r - r_0)$, i.e., a thin ring with a narrow tunnel junction, gives $J_0(r_0 k)$, a zeroth order Bessel function with maximum at $k = 0$. Similarly, a Fourier transform of $\delta(r - r_0) \exp{(i\theta)}$ yeilds $J_1(r_0 k)$, which is zero for $k = 0$.